

DYNAMICS OF WAKES DOWNSTREAM OF WIND TURBINE TOWERS

Melvin H. Snyder* and W.H. Wentz, Jr.*
 Wind Energy Laboratory
 Wichita State University
 Wichita, Kansas 67208

ABSTRACT

The near-field wakes downstream of circular cylinders and of 12-sided cylinders were surveyed in a wind tunnel. Local velocity and velocity deficit diagrams are presented. The variation of turbulence in the wake was surveyed and the frequency of the periodic component of wake motion was determined. Differences between wakes of circular cylinders and of 12-sided cylinders are discussed. Also effects of strakes, orientation of the 12-sided cylinders, and rounding of the corners are noted.

SYMBOLS	BACKGROUND
<p>D Diameter of cylinder (or of circumscribed circle)</p> <p>f Frequency of periodic component of wake motion</p> <p>N Number of samples taken at data point</p> <p>q Dynamic pressure, $1/2 \rho V_{\infty}^2$</p> <p>r Radius of curvature of corners of 12-sided cylinders</p> <p>R Cylinder radius = $D/2$</p> <p>Re Reynolds number = $\rho VD/\mu$</p> <p>S Strouhal number = fD/V_{∞}</p> <p>u_{mean} Average local velocity</p> <p>u u_{mean}</p> <p>u_x x-component of local velocity</p> <p>u'_{rms} Standard deviation (see text)</p> <p>u_1 $1 - (u_x/V_{\infty})$</p> <p>V_{∞} Freestream velocity</p> <p>x Streamwise distance downstream measured from centerline of cylinder to plane of survey in cylinder diameters</p> <p>y Distance along the cylinder axis</p> <p>z Distance normal to the x-z plane and measured from x-z plane passing through cylinder centerline</p> <p>z_R Half-width of wake</p> <p>α Orientation of 12-sided cylinder, see text</p> <p>σ Standard deviation = u'_{rms}</p>	<p>Wind turbine towers are often composed of cylinders, either as components of truss-type towers or as single column towers. Two types of towers and tower elements in use are circular cylinders and 12-sided cylinders. In the cases of turbines operating with rotors downwind of towers, there have been some undesirable results of the blades passing through the tower wake. These results include unwanted noise, as well as fluctuating loads on the blades resulting in transient torque and thrust loads.</p> <p>The wake produced by separation of the flow from a cylinder is marked by velocity deficiency, i.e., decreased kinetic energy, and by unsteady behavior. The unsteady behavior has two components--"turbulence," by its nature random; and a regular periodic part, described by Roshko as "organized motion." These "organized" vortices shed from the cylinder are superimposed on the background of general turbulence (reference 1 and 2).</p> <p>There is uncertainty regarding just what it is about the nature of the wake which causes the noise and other effects mentioned above, i.e., is it the (1) periodic structure of the wake, (2) velocity deficit, or (3) turbulence of the wake?</p> <p>To obtain a model of the wake, wind tunnel tests were conducted in the Walter Beech Memorial Wind Tunnel of Wichita State University. The tests were surveys of wakes downstream of circular cylinders and of 12-sided cylinders.</p>
	<h3>MODELS</h3> <p>Four models were tested. Two models were circular cylinders, 0.17 m (6.7 in.) diameter and 0.508 m (20 in.) diameter. There were also two 12-sided cylinders; the smaller had a diameter of circumscribed circle of 0.182 m (7.17 in.), and the larger had a 0.508 m (20 in.) diameter circumscribed circle. The smaller models were mounted horizontally across the 2.13 m x 3.05 m (7 x 10 ft) tunnel test section (Fig. 1), and the larger models were mounted vertically.</p> <p>The wake of the cylinders was surveyed at various stations downstream. Most published details regarding cylinder wakes are for long distances downstream (e.g., Schlichting: velocity deficit at greater than 50 diameters downstream--ref. 3;</p>

*Professors of Aeronautical Engineering

see also ref. 4). Most downwind wind turbine blades will be operating in the range of 3 to 6 diameters downstream of the centerline of the cylinder producing the wake. Surveys were conducted at stations in the range from 2 diameters to 9 diameters downstream of the cylinder centerlines.

INSTRUMENTATION AND DATA PROCESSING

Pressure Probe Survey

Two types of instrumentation were used. Pressure measurements were made using a 5-tube probe (Fig. 2) to determine local velocity. Pressure data were processed on-line to determine local velocity magnitude and direction and all components.

Hot-Film Anemometer

The second phase of testing of each model was a survey of the wake using a hot-film anemometer. Figure 3 diagrams this data system. Linearized voltage signals from the hot-film anemometer were fed directly into the minicomputer; 6000 measurements were made at each station at a rate of 400 Hz, for a total sampling time of 15 seconds. These data were processed in about 40 to 45 seconds per station.

Voltage measurements were digitized, stored, and converted to velocity values. The velocity values were processed to determine the sample mean and standard deviation (σ). The standard deviation of a velocity sample is the turbulence intensity, when non-dimensionalized by a reference velocity. Local turbulence intensity was calculated, based on local mean velocity, and global turbulence intensity was calculated based on the remote freestream velocity.

$$u_{\text{mean}} = \bar{u} = \frac{\sum_{i=1}^N u_i}{N} \quad [\text{m/s (fps)}]$$

where N is total number of samples.

$$\text{Standard deviation} = \sigma = u'_{\text{rms}} = \sqrt{\frac{\sum_{i=1}^N (u_i - \bar{u})^2}{N}} \quad [\text{m/s (fps)}]$$

$$\text{"Global Turbulence Intensity"} = \text{TI} = \frac{u'_{\text{rms}}}{V_{\infty}}$$

$$\text{"Local Turbulence Intensity"} = \text{TIL} = \frac{u'_{\text{rms}}}{\bar{u}}$$

Velocity distribution was determined using a method of bins. A series of seven bins are used for determination of the sample histogram. The central bins are of σ width, centered about the mean, and the 1st and 7th bins are the "tails" for data respectively below and above the central bins. The entire sample is sorted into these

bins to determine the distribution of the sample. The number printed for each bin is a fraction of the total number of samples.

Spectral Analysis

The signal from the hot-film anemometer was also fed to an analog spectrum analyzer (Hewlett-Packard model 3580A). Results were recorded in the form of photos of an oscilloscope trace of the power spectral density (psd). Figure 4 shows a typical photo obtained during these tests. For signals for which significant periodicity is present, the frequency or frequencies at which peaks in the psd appear are tabulated, non-dimensionalized, and presented in the form of Strouhal numbers ($S = fd/V_{\infty}$).

CIRCULAR CYLINDER TESTS

Testing

The smaller (0.17 m dia.) cylinder was mounted horizontally as shown in Figure 1. The wake was surveyed at stations $x = 300\%$, 450% , 600% , 750% , and 900% using the 5-tube pressure probe. Measurements were taken every half-inch from $z = -10$ inches to $z = +10$ inches. Tunnel dynamic pressures ranged from 8.14 N/m^2 to 3.11 kN/m^2 providing Reynolds numbers from 174000 to 758000.

Survey of the wake using the hot-film anemometer was performed completely at $x = 300\%$ and for a more limited number of z -positions at the other stations. Frequency of the periodic component of the wake was determined at all stations and for a complete range of Reynolds numbers.

Two sets of spiral strakes were attached to the 17 cm circular cylinder and the wake was surveyed using the 5-tube probe at stations $x = 300\%$ and 600% . The strakes were fabricated from sheet aluminum, were 1.6 cm high (approximately 10% of diameter), and made an angle of 30° with the cylinder centerline (Fig. 5). Initial testing was done with the strakes in the 90° position in the plane of the survey (x - z plane), as in Figure 5. The cylinder was rotated 90° on its axis putting the strakes at the 0° and 180° position, in the plane of survey.

The large (0.508 m dia.) circular cylinder was tested only briefly after all of the 12-sided cylinder tests had been completed. It was mounted vertically in the wind tunnel to provide as much clearance between the cylinder and side wall as possible. Only the hot-wire anemometer was used at $x = 300\%$.

Test Results

The results presented in Figures 6 and 7 are only sample runs. Complete results are presented in References 5 and 6.

Reversed flow, which results from separation of the boundary layer from a circular cylinder, was not found to be present in the range of 3 to 9 diameters downstream at any of the test Reynolds numbers ($.17 \times 10^6 < Re < .76 \times 10^6$). Apparently the reversed flow region is confined to the region between the cylinder and the $x = 300\%$ station (Fig. 6).

Figure 7 more clearly shows the nature of the velocity defect in the wake. u_1 is plotted at five stations in the wake, where $u_1 = 1 - (u_x/V_\infty)$. As expected, the velocity deficit profile is affected by the nature of the separation from the cylinder. Critical Reynolds number is approximately 400,000. At less than critical Reynolds number, the laminar boundary layer separates at about the 90° position on the cylinder. At greater Reynolds numbers the boundary layer is turbulent and separates downstream of the 90° point resulting in a narrower wake which should be characterized by more turbulence but with a smaller velocity deficit at a given station because of the more effective mixing in the wake.

Figure 8 summarizes these expected effects of Reynolds number on the velocity deficit profiles at $x = 300\%$ and 750% . Note that at Reynolds number of 420,000, the wake is not symmetrical on the centerline. This lack of symmetry is apparently due to turbulent separation on one side and laminar separation on the other side of the cylinder. Apparently there was a small difference in the cylinder smoothness so that critical Reynolds number was slightly different for the two sides. Oil dot tests to visualize the separation point appeared to confirm unsymmetrical separation at about $Re = 0.42 \times 10^6$.

The shape of the wake velocity defect was non-dimensionalized by plotting u_1/u_{1max} vs. z/z_R , where z_R is the semi-width of the wake. The resulting profiles are compared in Figure 9 with the profile which Schlichting defines at a long distance downstream (greater than 50 diameters--see ref. 3). Figure 9a is for the subcritical wake ($Re = .17 \times 10^6$), and Figure 9b is the profile at $Re = .76 \times 10^6$. The non-dimensional profiles are quite sensitive to the wake width which is chosen. In both cases the profile approaches the "standard shape" as the wake progresses downstream.

Growth of the wake is indicated in Figure 10. The locus of 50% u_{1max} position spreads at an included angle of about 3° (1.5° to centerline) for the subcritical wake. The supercritical wake (Fig. 10b) starts narrower and the 50% u_{1max} lines diverge at only about 2 degrees.

Turbulence intensity is plotted at the $x = 300\%$ station for various cylinder Reynolds numbers in Figure 11. Highest levels of turbulence correspond to high subcritical Reynolds numbers. It is also apparent that turbulence intensity has a double peak--corresponding to the mixing regions. Highest turbulence intensity corresponds to highest $(\partial u/\partial z)$ and lower values of turbulence are at $(\partial u/\partial z) \rightarrow 0$ (at the center of the velocity deficit profile and at the edges of the wake).

Turbulence intensities are mapped in Figures 12a and 12b.

As described above, a periodic structure is superimposed on the general turbulence of the wake (or vice-versa). The frequency of this periodic structure is represented in Figure 13 by Strouhal number, where Strouhal number = $S = (fD/V_\infty)$. The variation of Strouhal number with Reynolds number

agrees very well with that reported by McCroskey (ref. 2), i.e., below critical Reynolds number, $S \approx 0.2$; above $Re = 400,000$, S increases to greater than 0.4.

In Reference 1, Roshko illustrates the tendency for vortices in a wake to combine, stretching the length of the periodic structure as it moves downstream. This action should change the frequency of the wake in a way which may be significant to the perceived noise of the wake. Figure 14 indicates some shift in the wake frequency as the instrumentation is moved downstream.

When strakes were added, two important results were noticed. The reversed flow (deadwater) region was increased in size extending beyond the 300% station when the strakes were at $\pm 90^\circ$ (in plane of measurements--see Fig. 15a). Also, the periodic structure of the wake was weaker, or else the general turbulence was stronger, so that any periodic motion was completely immersed in the random turbulence so that no dominant frequency could be measured.

The fact that the reversed flow region extended beyond the 300% station downstream of the $\pm 90^\circ$ strakes (Fig. 15b) but did not reach 300% downstream of strakes at 0° and 180° , indicates that spiral strakes produce a fairly strong 3-dimensional motion to the wake.

12-SIDED CYLINDER TESTS

Testing

The mounting and testing of the 12-sided cylinders was the same as that of the circular cylinders. The large [0.508 m (20 in.) dia. circumscribed circle, 0.491 m (19.32 in.) dia. inscribed circle] cylinder was tested first. It was immediately obvious that the periodic component of the wake was quite strong. The buffeting wake forced the tunnel dynamic pressure to be limited to less than 1 kN/m^2 to prevent structural damage to wind tunnel control room windows. Similarly, the strength of the periodic component of the wake of the smaller [18.2 cm (7.17 in.) dia. circumscribed circle, 17.7 cm (6.95 in.) dia. inscribed circle] 12-sided cylinder was greater than for the similar sized circular cylinder. The dynamic pressure of those tests was limited to 2.15 kN/m^2 because of model and test section wall vibration. Table I lists test ranges.

TABLE I 12-SIDED CYLINDER TESTS

Dynamic Pressure, q [N/m ² (psf)]	Reynolds Number	
	(Large Cylinder)	(Small Cylinder)
71.8 (1.5)	0.52×10^6	0.19×10^6
143.6 (3.0)	0.72×10^6	---
87.3 (6.0)	0.98×10^6	0.36×10^6
574.6 (12.0)	1.32×10^6	0.49×10^6
957.6 (20.0)	1.59×10^6	0.60×10^6
1436.4 (30.0)	---	0.68×10^6
2154.6 (45.0)	---	0.77×10^6

The cylinders were tested in two positions with respect to freestream wind direction. With flat sides parallel to the freestream direction (i.e., a flat at the stagnation point) the position was defined as $\alpha = 0^\circ$. Rotated 15° , with a point at the stagnation point, the position was defined as $\alpha = 15^\circ$.

Following testing of the small 12-sided cylinder with sharp corners, it was modified to permit testing with rounded corners to simulate production utility poles. Two sizes of round corners were tested: small radius corners, $r = 8.4$ mm, $r/R = 4.6\%$, and large radius corners, $r = 16.8$ mm, $r/R = 9.2\%$.

Test Results

The complete set of wake velocity diagrams and velocity-deficit diagrams are presented in Reference 5; Figures 16 and 17 are representative of the results. The reversed flow region is upstream of $x = 200\%$ and considerable velocity recovery occurs between the 200% and 300% stations. Wake growth is shown in Figures 18 and 19. Apparent from these figures is a higher rate of spreading than in the case of a circular cylinder.

Also, the nature of the wake and the rate of wake spreading is more affected by orientation of the cylinder than by Reynolds number. On a circular cylinder the nature of the boundary layer (laminar or turbulent, energy level, etc.) is a function of the Reynolds number. Because of this dependency, the point of boundary layer separation is a function of the Reynolds number; the point of separation is the primary factor affecting the wake geometry.

In the case of the 12-sided cylinder (probably any cylinder having a polygon cross-section), the point of separation is fixed by the corner, not primarily by Reynolds number. The corner, which produces an adverse pressure gradient, will be the point of separation. Thus, the geometry of the wake is fixed by geometry, and is relatively insensitive to Reynolds number. This hypothesis is reinforced by the graph of the Strouhal number presented in Figure 20. The Strouhal number is not a function of Reynolds number; it is approximately constant for given orientation. Turbulence intensity of the 12-sided cylinder wake is of the same order of magnitude as that of the wake of a circular cylinder. However, the strength of the periodic component of the wake motion is much greater for the 12-sided cylinder than for the circular cylinder.

Rounding the corners of the 12-sided cylinder produces two effects: (1) the strength of the periodic component of wake motion appears to be reduced (observed qualitatively, not measured), (2) some dependency on Reynolds number is produced (see Fig. 21).

SUMMARY OF RESULTS

The results may be summarized:

1. The wake downstream of a cylinder has three characteristics which may affect a wind turbine

blade passing through the wake:

- a. A velocity deficit compared to the freestream wind,
 - b. Random turbulence of wide frequency range and moderate strength,
 - c. Low frequency (less than 100 Hz) periodic vibrations.
2. The velocity deficit profile for the near-field is different than the published far-field profiles (e.g., ref. 3).
 3. The turbulence associated with the mixing has highest values on both sides of the wake centerline, where (du/dz) values are highest.
 4. The magnitude of turbulence is about the same for 12-sided cylinders as for circular cylinders.
 5. The strength of the periodic component of the wake structure is greater for a 12-sided cylinder than for a circular cylinder.
 6. The separation point and geometry of the wake of a 12-sided cylinder is independent of Reynolds number (unlike a circular cylinder).
 7. Rounding the corners of the 12-sided cylinder causes some dependence on the Reynolds number and reduces the strength of the periodic motion.
 8. Spiral strakes on a circular cylinder can eliminate the periodic motion of the wake-- at the expense of increased velocity deficit and turbulence of the wake.

REFERENCES

1. Roshko, A.: "Structure of Turbulent Shear Flows: A New Look," Dryden Research Lecture, AIAA Journal, vol. 14, no. 10, October 1976.
2. McCroskey, W.J.: "Introduction to Unsteady Aspects of Separation in Subsonic and Transonic Flow," AGARD.
3. Schlichting, H.: Boundary Layer Theory, McGraw-Hill, New York.
4. Schetz, J.A.: Injection and Mixing in Turbulent Flow, Volume 68, Progress in Astronautics and Aeronautics, AIAA, 1980.
5. Snyder, M.H., and Wentz, W.H., Jr.: "Characteristics of the Wakes Downstream of Circular Cylinders and 12-Sided Cylinders, as Determined by Wind Tunnel Tests," WER-13, Wind Energy Laboratory, Wichita State University, January 1981.
6. Snyder, M.H., and Wentz, W.H., Jr.: "Wind Tunnel Data--Characteristics of Wakes of Circular Cylinders and 12-Sided Cylinders," WER-13A, Wind Energy Laboratory, Wichita State University, January 1981.

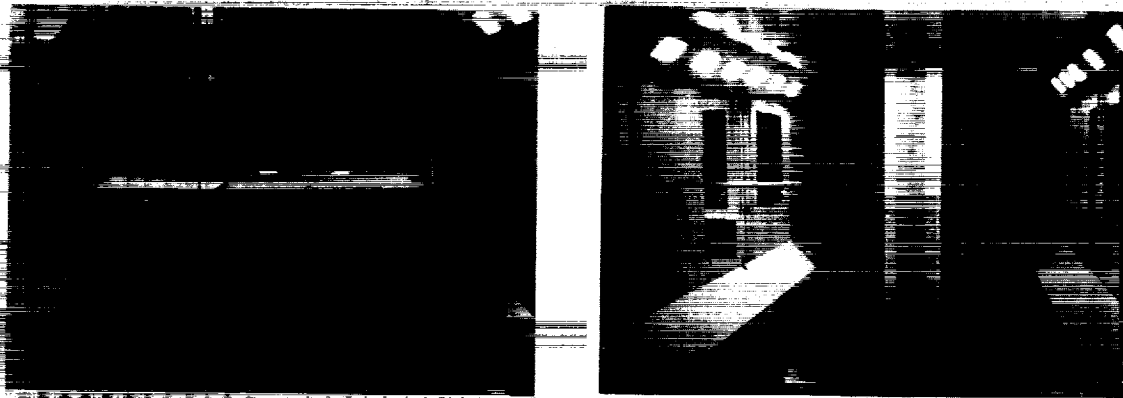


Fig. 1. Cylinders Mounted in Wind Tunnel.

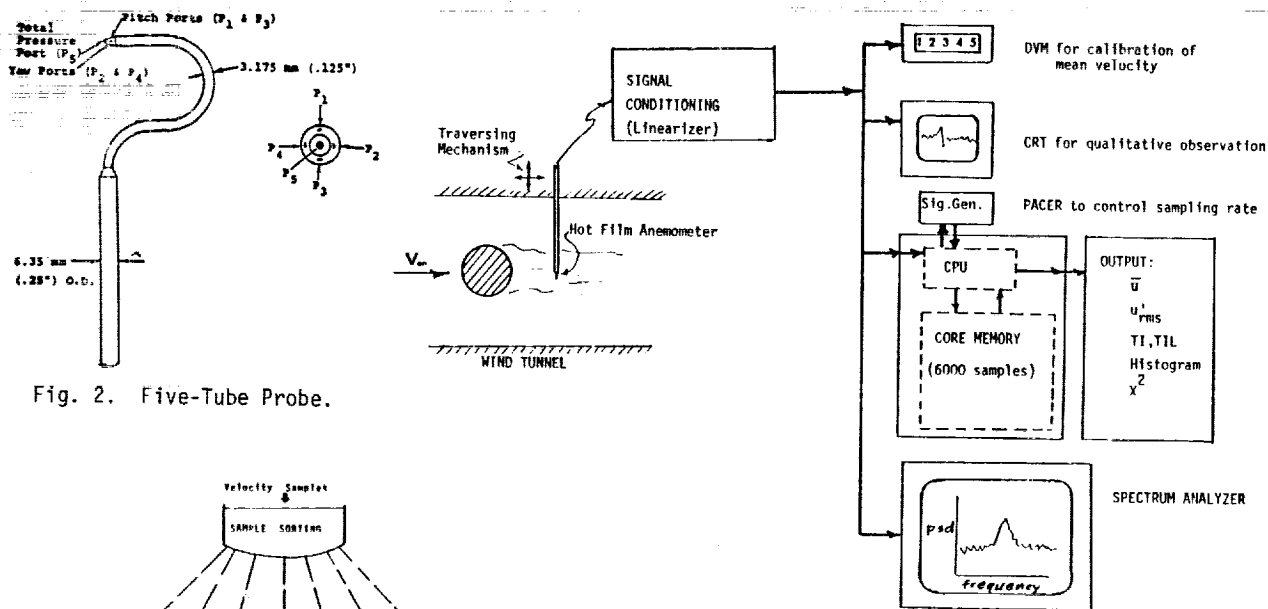


Fig. 2. Five-Tube Probe.

Fig. 3a. Hot Film Data Processing System.

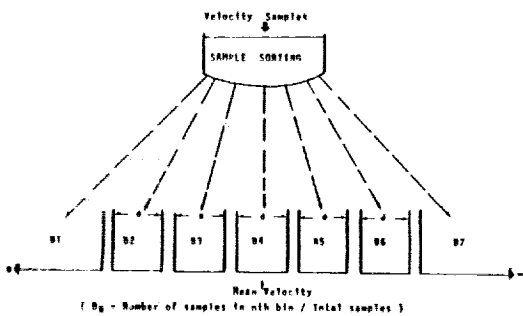


Fig. 3b. Method of Bins.

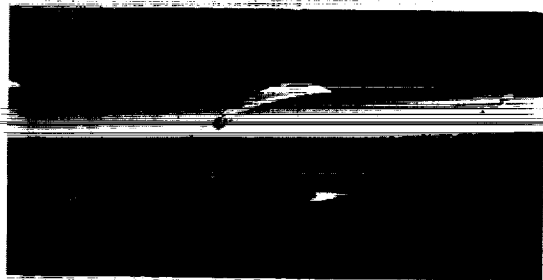


Fig. 5. Strakes on Circular Cylinder.

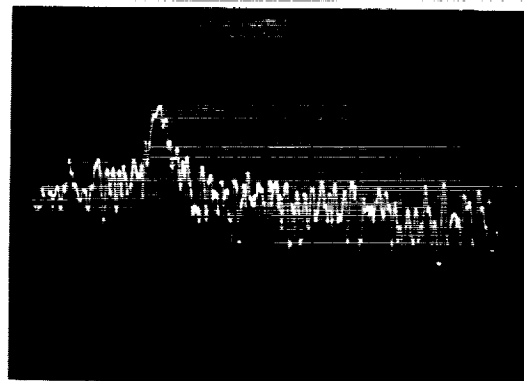


Fig. 4. Typical Spectrum Analyzer Output.

CIRCULAR CYLINDER

September 1980

$q = 7.5 \text{ psf}$ Diameter = 6.7 inches

$R.N. = 0.342 \times 10^6$

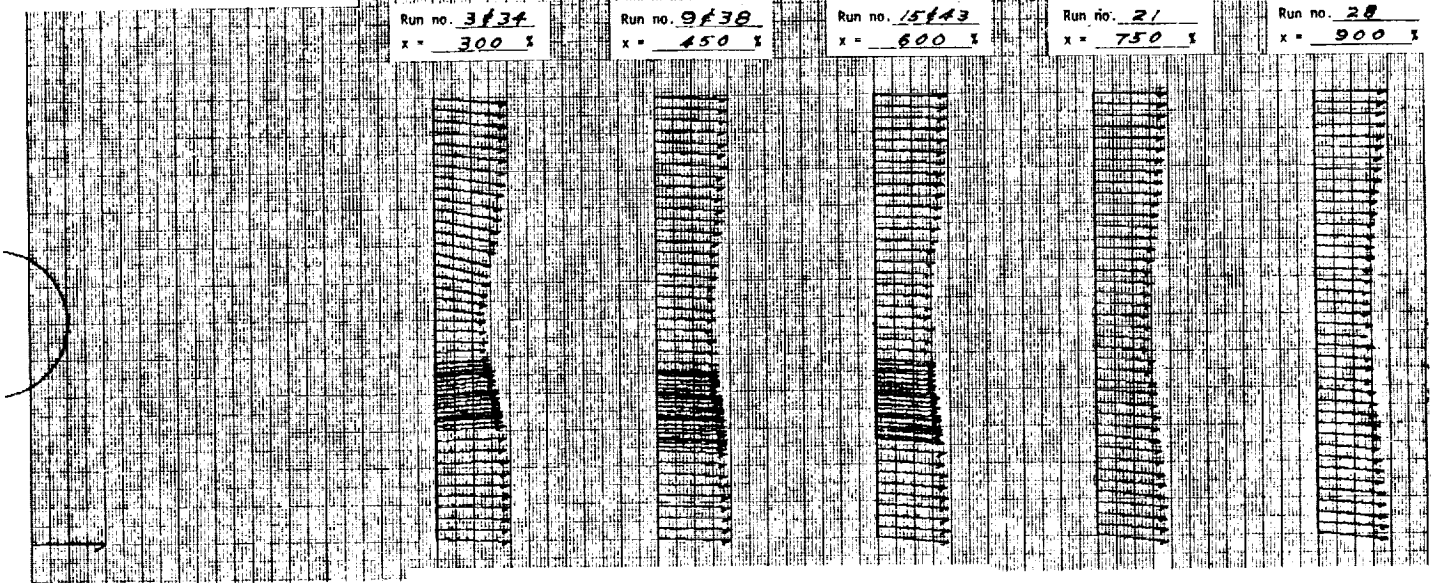


Fig. 6. Representative Wake Velocity Patterns.

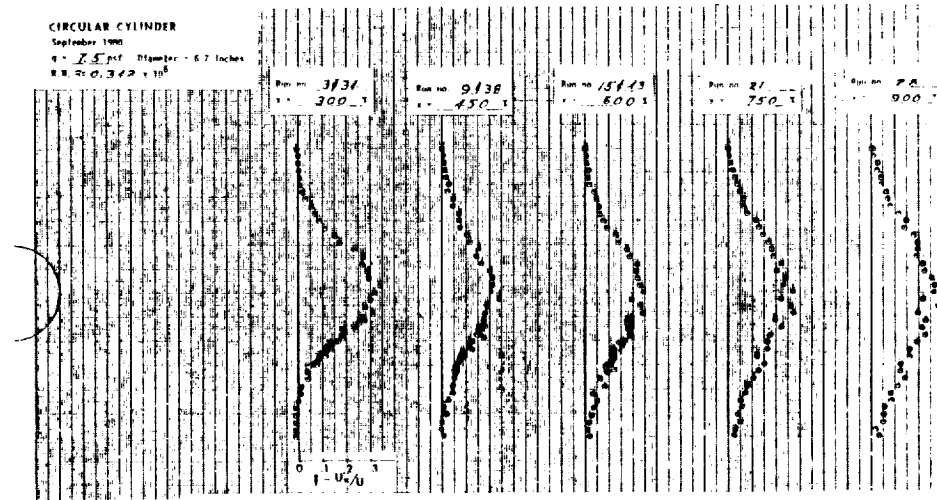


Fig. 7. Representative Wake Velocity Deficits.

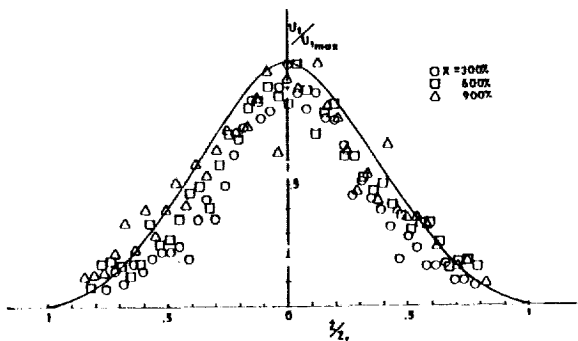


Fig. 9a. Wake Compared to Schlichting's Standard, $Re = 0.17 \times 10^6$.

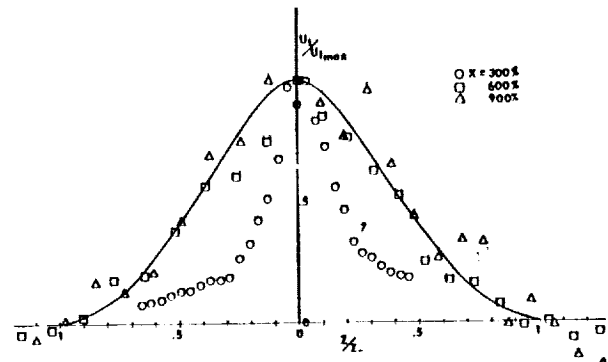


Fig. 9b. Wake Compared to Schlichting's Standard, $Re = 0.76 \times 10^6$.

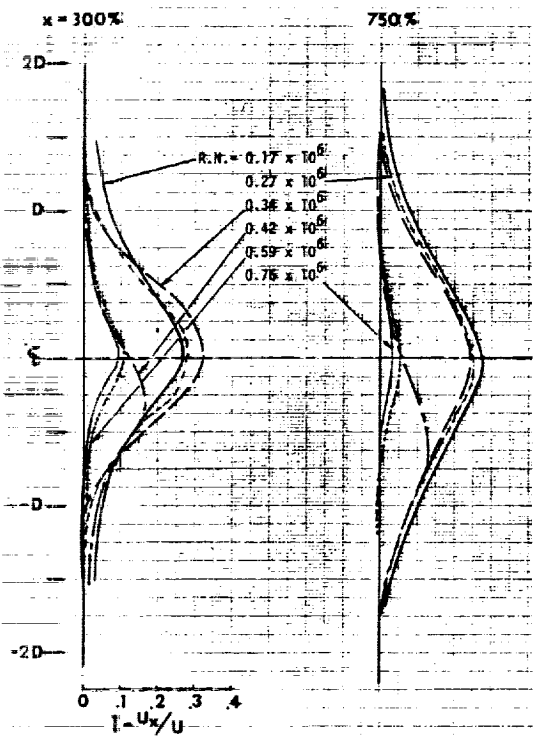


Fig. 8. Circular Cylinder Wake Velocity Deficits.

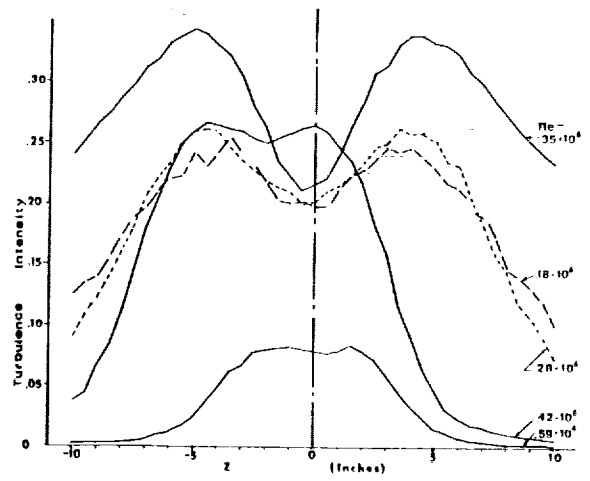


Fig. 11. Circular Cylinder Wake Turbulence Intensity at $x = 300\%$.

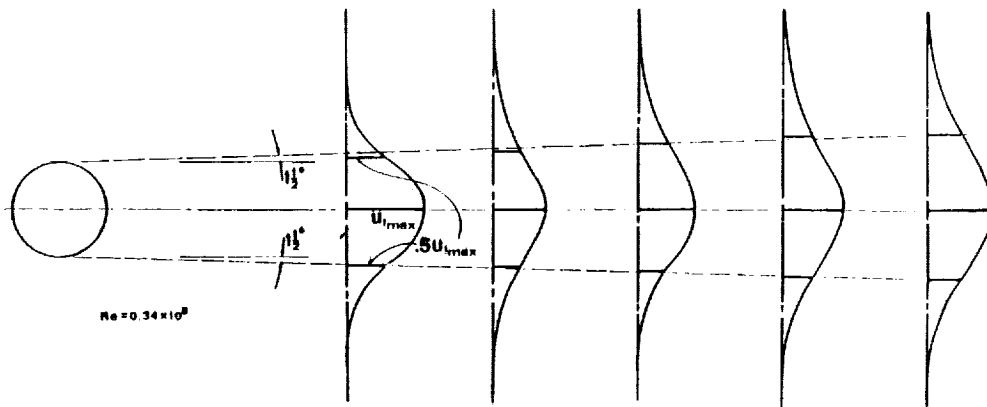


Fig. 10a. Subcritical Wake Growth.

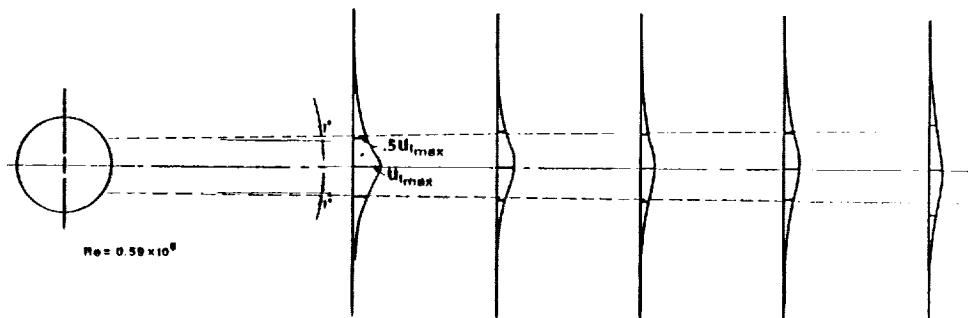


Fig. 10b. Supercritical Wake Growth.

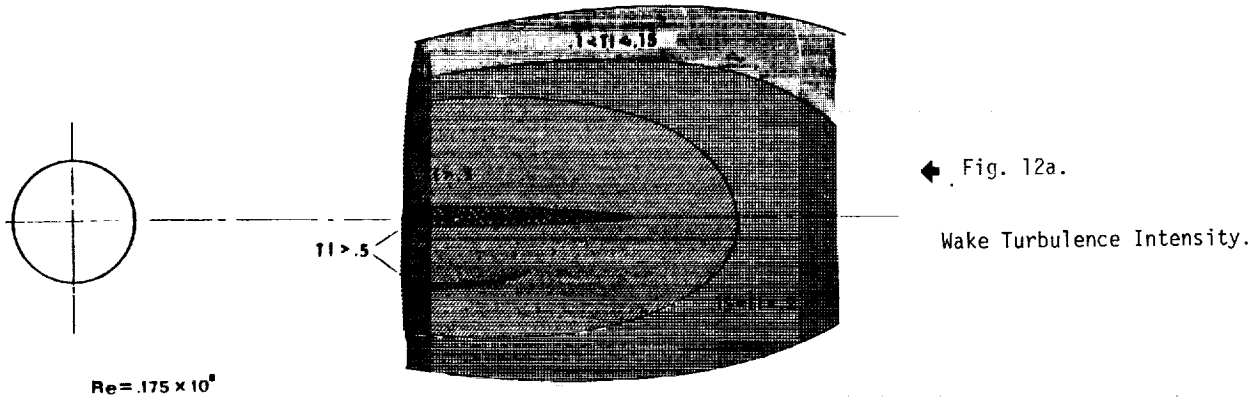


Fig. 12b. →

Wake Turbulence Intensity.

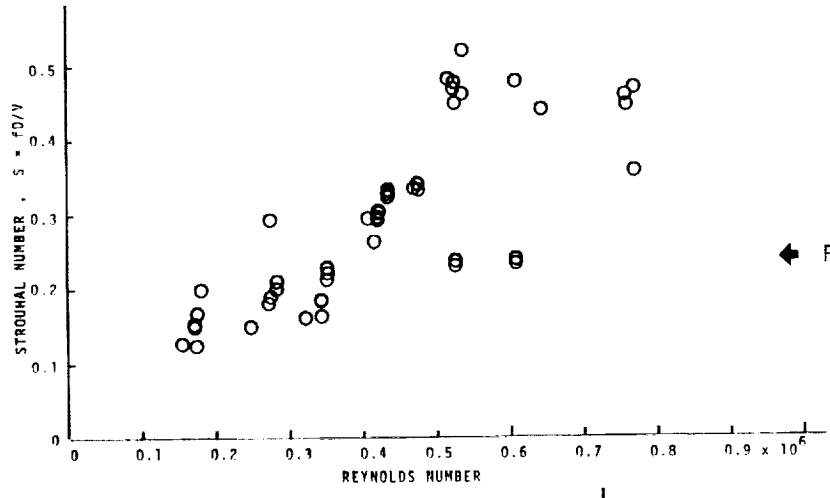
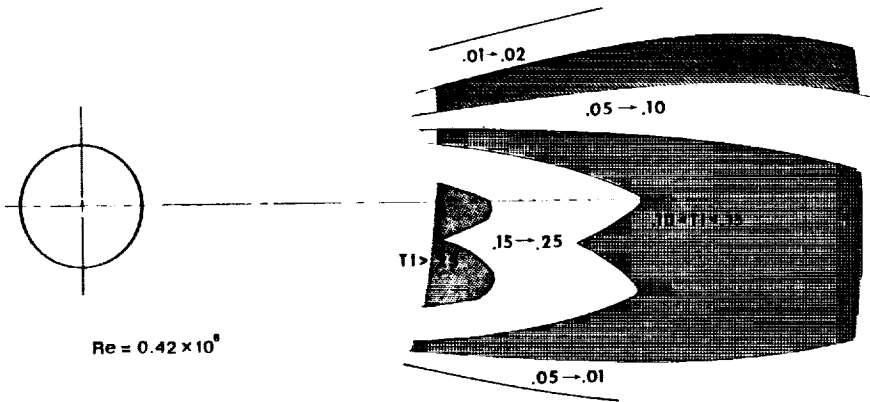
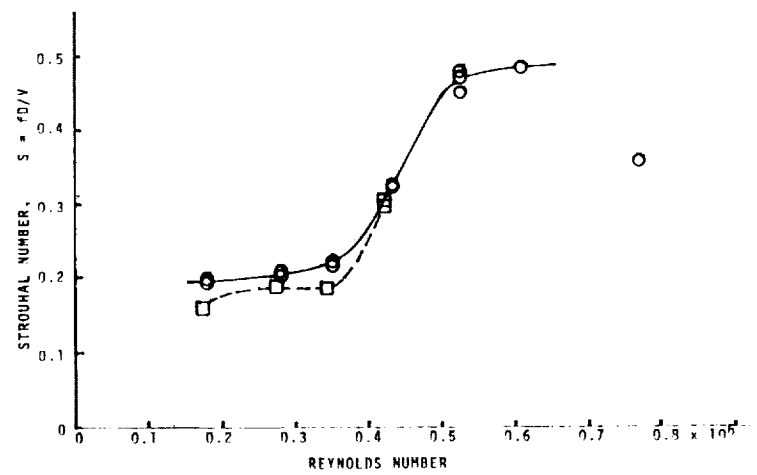


Fig. 14. →

Circular Cylinder Wake. Solid curve is at $x = 300\%$, dotted curve at $x = 600\%$.



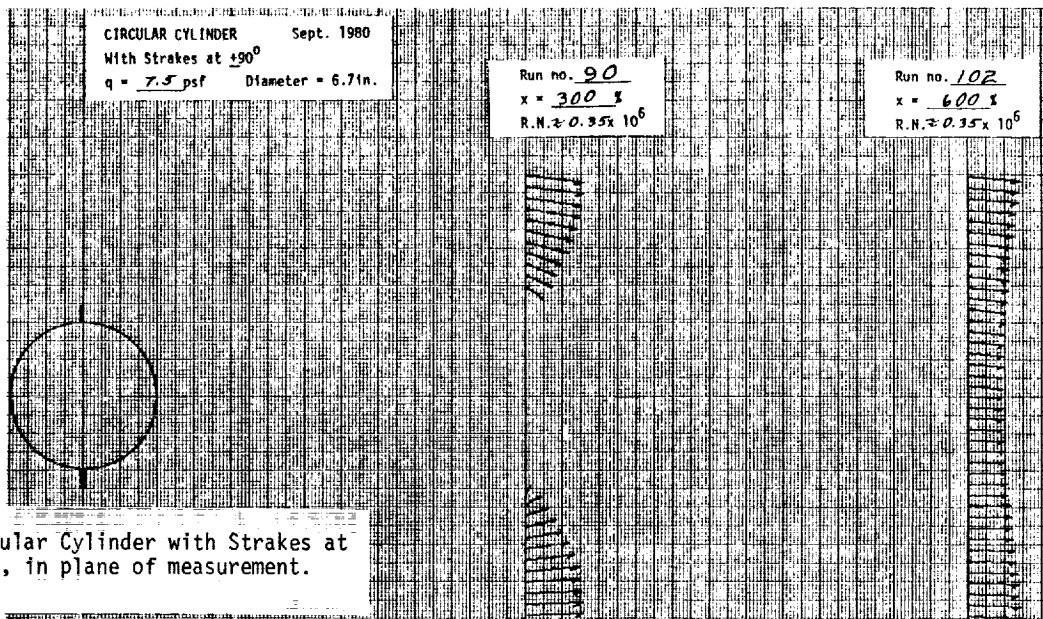


Fig. 15a. Circular Cylinder with Strakes at $\pm 90^\circ$, in plane of measurement.

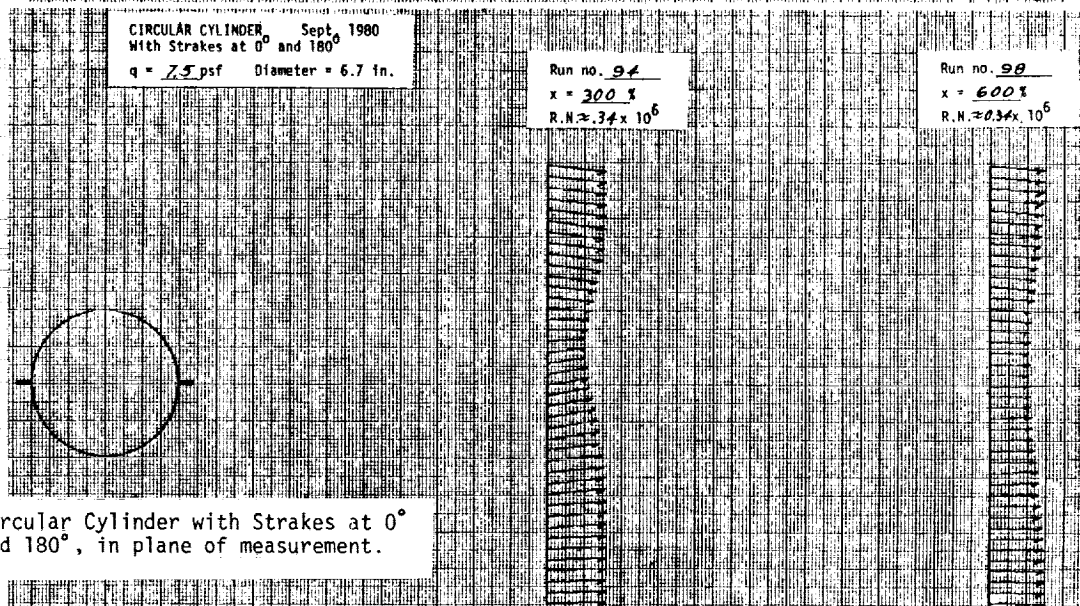


Fig. 15b. Circular Cylinder with Strakes at 0° and 180° , in plane of measurement.

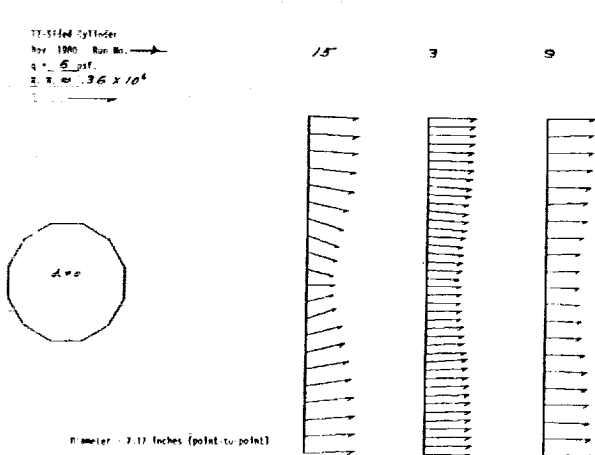


Fig. 16. Velocity Pattern Example.

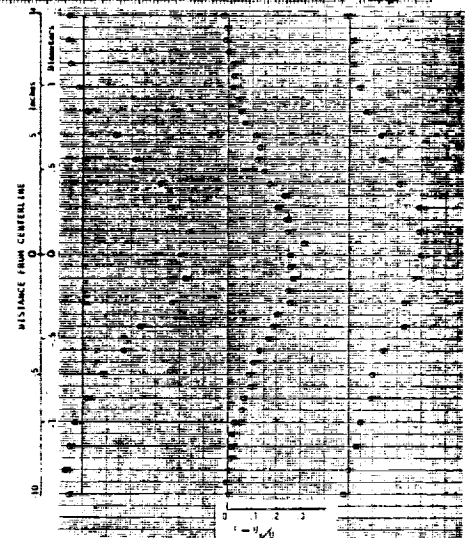


Fig. 17. Velocity Deficit Example.

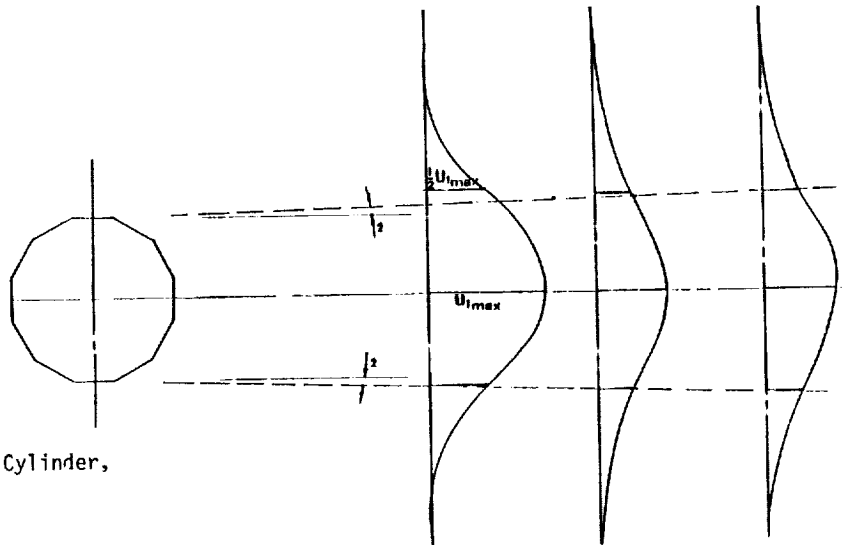


Fig. 18. Wake Spreading, 12-Sided Cylinder, $\alpha = 0$, $Re = .36 \times 10^6$.

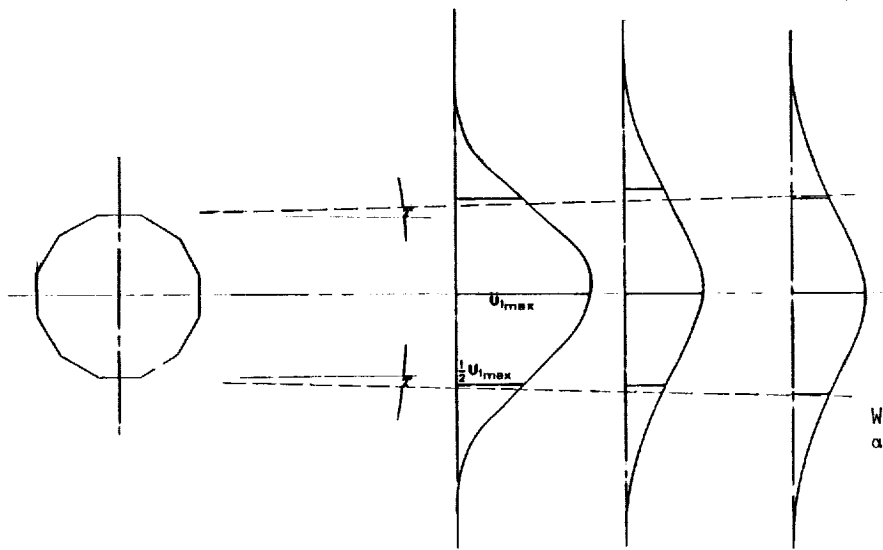


Fig. 19.

Wake Spreading, 12-Sided Cylinder, $\alpha = 0$, $Re = .59 \times 10^6$.

Fig. 20. Strouhal Number for 12-Sided Cylinder.

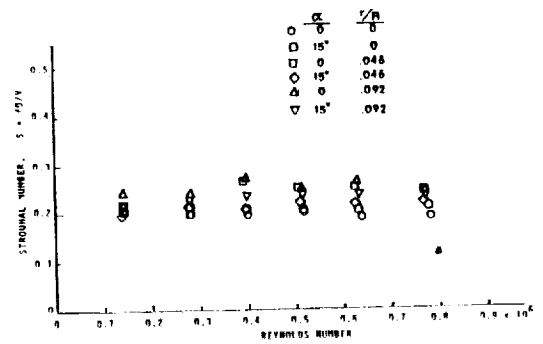
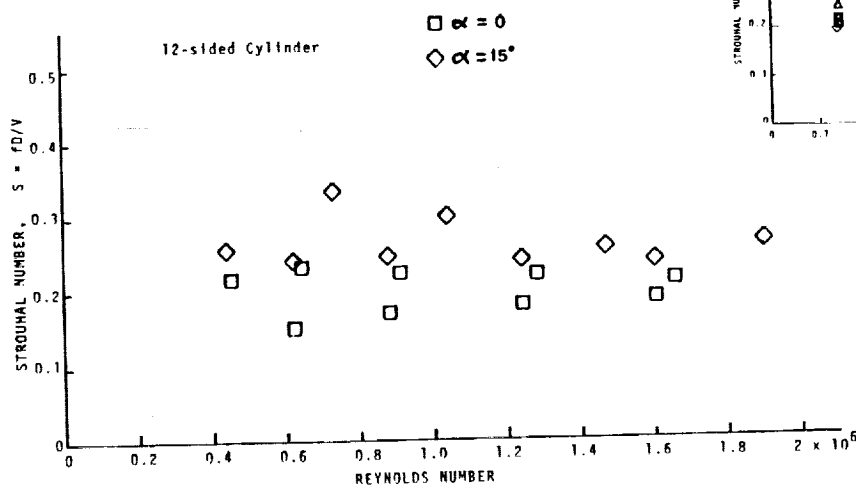


Fig. 21.

Effects of Rounding Corners

QUESTIONS AND ANSWERS

M.H. Snyder

From: R. Spencer

Q: What maximum wake deficit was found downstream of the circular cylinder?

A: *Maximum value of $1 - u_x/u$ was 1 at the end of the reversed flow region. Had we used a double-film anemometer we could have made measurements in the reversed flow region (possibly as high as 1.2). The high deficiency region smooths out rather quickly--in most cases, by 3 cylinder diameters downstream.*

From: A.C. Hansen

Q: Can you comment on the importance of free stream shear and turbulence to the periodic vortex shedding?

A: *No, we made no measurements in sheared flow. All tests were in the wind tunnel which has a relatively low turbulence factor.*

Some years ago, some of my students worked on problems of pressure distribution on cylinders in sheared-flow fields (analytically and experimentally). There was significant alteration of pressure distribution and streamline pattern. Therefore, I expect that shear will affect vortex shedding. I have not yet tried to apply these results to this problem.

From: Anonymous

Q: Was the low frequency periodic vibration measured on a circular cylinder related to the Strouhal vortex shedding frequency at that Reynolds number?

A: *Yes.*

From: Anonymous

Q: Did you vary the height of the strakes and what is the typical ratio of strake dimension to diameter?

A: *No, we only had time to test one set of strakes, 0.10 high. I plan to do further testing.*

